Title

Analysis of Defect Irrelevancy in a Non-Insulated REBCO Pancake Coil Using an Electric Network Model

Journal

IEEE Transactions on Applied Superconductivity, 32(6)

ISSN

1051-8223

Authors

Webb-Mack, Zo

Ji, Qing

Wang, Xiaorong

Publication Date

2022

DOI

10.1109/tasc.2022.3171164

Analysis of Defect Irrelevancy in a Non-Insulated REBCO Pancake Coil Using an Electric Network Model

Zoë Webb-Mack, Qing Ji, and Xiaorong Wang

***Abstract*—High-temperature superconducting REBCO coated conductor is one of the main candidates for next-generation high field magnets in fusion reactors and particle accelerators owing to their high current-carrying capability. Although these materials can operate at higher temperatures and generate higher magnetic fields than their counterparts with lower critical temperatures, protecting the REBCO magnet against quench is challenging. A variety of candidate technologies that may be able to enable self-protection, including no-insulation technology and insulative coatings with temperature-dependent resistance, are in development. In order to understand current sharing and thermal processes during a quench, we model a REBCO pancake coil as an electrical circuit, considering power generation and heat transfer along conductor turns, and study the current distribution around a local defect with lower critical current. The magnetic field and coil terminal voltage predicted by the simulation was compared to published experimental results. Our results provide useful insights into how current sharing occurs around defects.**

***Index Terms*—Circuit simulation, high-temperature superconductors, superconducting magnets.**

I. Introduction

HIGH-TEMPERATURE superconductors (HTS), which can operate above the temperature of liquid helium, 4.2 K, are needed in order to achieve powerful magnetic fields required for applications in next-generation fusion power and particle colliders. Although low-temperature superconductors (LTS) already in use (like Nb_3Sn) can achieve fields approaching 16 T at 4.2 K, more powerful fields at around 20 T and higher are desired and high temperature superconductors (HTS) are required [1], [2]. Additionally, low-temperature superconducting magnets are usually cooled using liquid helium, posing a significant demand in cryogenic refrigeration power.

One such HTS material is rare-earth barium-copper oxide (REBCO), which has a critical temperature of around 92 K. In application, REBCO pancake coils where REBCO tapes wound in a spiral to form a disk-like structure are stacked to form a solenoid magnet. Of particular concern is quenching, during which stored magnetic energy is converted into heat and the superconductor transitions into its "normal" (non-superconducting) state [3]. Since the heating process can damage the coil, it is important that HTS systems are protected against quenching.

One way to achieve self-protection is to encourage current sharing between conductor turns. If there is a local defect with lower critical current or a local hotspot (also called a "normal zone"), low resistance between turns allows the current to bypass the defect or hotspot and prevent potential overheating. No-insulation (NI) technology, in which no insulation is placed between conductor turns, is one way to achieve this current sharing [4]. Although the no-insulation REBCO magnets demonstrate strong self-protection capability and superior field generation [5], they show significant charging delay, strong eddy currents and field distortion during charging [4]. These features may not be acceptable for applications that require precise magnetic fields during ramping such as particle accelerator magnets.

To address these potential drawbacks of the no-insulation REBCO magnet technology, a complete understanding of the electromagnetic behavior of the current sharing between conductor turns is required. Of particular interest is current sharing around defects in the HTS material, such as those caused by local quenching. Experimental data on current and heat distribution in the coil are limited due to constraints on how voltage taps and Hall sensors may be placed in experiments. There are only limited reports on the detailed distribution of current or heat generation within a coil [6]. In order to fully understand the behavior of the REBCO system and current distribution around defects we need to rely on simulation tools [7].

Here, we follow the idea of an equivalent electrical circuit [8]–[16] in the form of a rectilinear schematic [12] and expand our previous work on a stack of tapes [17], [18] by adding a

Manuscript received 30 November 2021; revised 10 March 2022; accepted 22 March 2022. Date of publication 28 April 2022; date of current version 19 August 2022. This work was supported in part by the U.S. Department of Energy, Office of Science, Office of Workforce Development for Teachers and Scientists (WDTS) under the Science Undergraduate Laboratory Internship (SULI) program, and in part by the U.S. Department of Energy, Office of Science, Office of High-energy Physics, through the US Magnet Development Program and Office of Fusion Energy Sciences under Contract No. DEAC02-05CH11231. *(Corresponding author: Zoë Webb-Mack.)*

Zoë Webb-Mack was with Lawrence Berkeley National Laboratory, Berkeley, CA 94720 USA. She is now with Duke University, Durham, NC 27708 USA (e-mail: zoe.webb-mack@duke.edu).

Qing Ji is with Fusion and Ion Beam Technology Program, Lawrence Berkeley National Laboratory, Berkeley, CA 94720 USA (e-mail: qji@lbl.gov).

Xiaorong Wang is with Superconducting Magnet Program, Lawrence Berkeley National Laboratory, Berkeley, CA 94720 USA (e-mail: xrwang@lbl.gov).

TABLE I
MAIN MATERIAL PARAMETERS USED IN THE MODEL

Parameter	Unit	Value
n, index value		33
Coil height [4]	mm	4.1
Coil inner radius [4]	mm	20.0
I_c at 77 K	A	68.2
E_c	μV/m	100
Contact resistivity	nΩ/m^2	1.0
ρCu at 77 K	nΩ·m	2.0
t_{tape}	mm	0.1
t_{Cu}	μm	40
t_{HTS}	μm	1.0

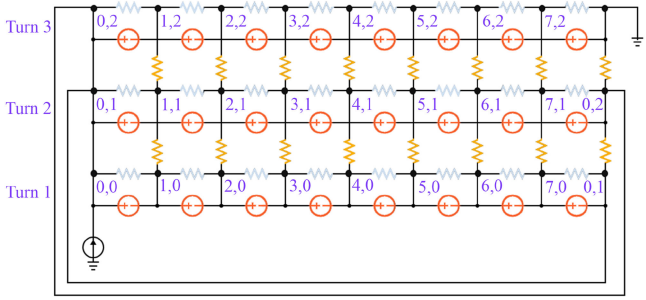

Fig. 1. Rectilinear schematic of three-turn coil with eight sections. Tape layers are represented as discrete components in parallel. HTS is represented as voltage sources (orange); contact resistance between layers is represented as radial resistors (yellow); and the copper stabilizer is represented as resistors (blue). The last node of each turn is equivalent to the first node of the next turn in order to preserve periodicity of the original circular geometry.

thermal simulation and validating it using experimental results. Our results using this model provide useful insights into how current sharing occurs around a local defect or normal zone: a defect in one turn of the coil affects azimuthal current flow in both the turn preceding and the turn following the defect. This behavior contrasts assumed current distribution around a defect.

II. ELECTRICAL NETWORK MODEL

A. Electrical Network Model of a REBCO Pancake Coil

In order to study the behavior of the REBCO pancake coil, we use NGSPICE [19] to simulate the pancake coil system as a circuit. NGSPICE netlists represent the circuit and are generated using a Python program that takes the geometric and electrical properties of a REBCO coil as input parameters, shown in Table I.

The coil is a spiral [8], so we imagine unfurling the spiral in order to model the coil as a rectilinear circuit. Fig. 1 shows how the coil is represented as a circuit. Periodic boundary conditions and resistance calculations based on the original circular geometry are implemented in order to maintain the integrity of the coil's physical geometry. Each turn of the coil (modelled as a row) is divided into sections so that each of the layers of REBCO tape may be modelled as a set of discrete components. Voltage sources represent the HTS layer and are given by $V = V_0\,[I/I_c]^n = E_0 * l[I/I_c]^n$, where V_0 is the voltage criterion, E_0 is the electric field criterion, l is the arclength of the section of tape, and I_c is the critical current of the REBCO layer and n is the index value. Table I lists the primary material parameters for the coil and tape used in the model. Resistors placed azimuthally represent the copper stabilizer according to $R_{Cu} = (\rho_{Cu} * l)/(t * w)$, where ρ_{Cu} is the electrical resistivity of copper, l is the arclength of the section of tape, t is the thickness of the copper layer, and w is the width of the tape (referred to as the "coil height" in Table I). Resistors placed radially represent contact resistance between turns according to $R_{radial} = \rho_{radial}/(l * w)$, where ρ_{radial} is average contact resistivity, l is the arclength of the section of tape, and w is the width of the tape. The radial resistance can be manipulated in future study to represent various electrical contact conditions.

NGSPICE runs a direct current ("dc") analysis over a sweep of transport currents, specified by the user, and outputs current through each component and voltage through each node. In order to accommodate NGSPICE's numerical constraints and avoid a numerical convergence error, if current through an HTS component is high, defined as $I/I_c > 5$, an HTS voltage source is swapped for a 1 GΩ resistor to approximate complete quench at that component's section. Using output data from NGSPICE, we calculate the magnetic field strength at the center of the coil under various conditions using the Biot-Savart law.

B. Thermal Simulation

We use the above network representation of a pancake coil to simulate heating in the coil over time. At each timestep over a user-specified interval, we account for temperature rise due to Joule heating by considering the power generation in each layer of the tape. A volumetric average of the Cu, REBCO and Hastelloy layers' heat capacity is used to determine temperature rise and heat diffusion between neighboring sections of tape along the same turn: $T_i^{j+1} = T_i^j + \alpha\Delta t/l^2[T_{i+1}^j - 2T_i^j + T_{i-1}^j]$, where T is temperature, α is the coefficient for thermal diffusion, l is the arclength of the section (the same for components all the same turn), superscripts indicate time step, and subscripts indicate the section in question. The specific heat of major components in the REBCO tape can be found in [20].

Adiabatic conditions are assumed: no heat exchange with the cryogen is considered. After updating the temperature distribution in the coil, the critical current, I_c, distribution is updated following a linear approximation of the temperature-dependent I_c between the operation temperature of 77 K and the critical temperature of 92 K. This process is run in steps of 0.25 s (which we found optimized run time while ensuring convergence). Time-dependent operating current was implemented in some runs to simulate current ramping.

III. RESULTS AND DISCUSSION

To test the model's validity, we compare simulated data for a 99-turn no-insulation coil to experimental results from [21], which studies the effect of defects in REBCO tape on magnetic field. We also compare simulated data for a 30-turn no-insulation

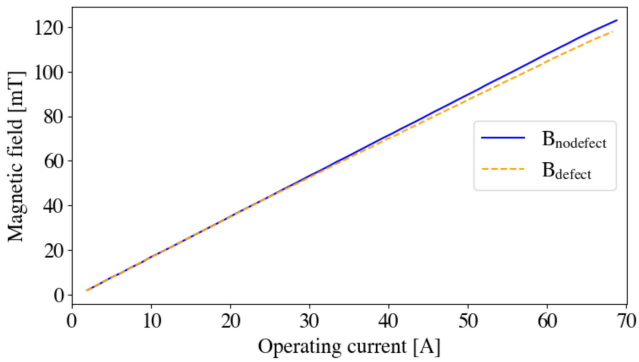

Fig. 2. Simulated data using the proposed electrical model demonstrates the negligible impact of six defects on the magnetic field produced by a 99-turn pancake coil for currents below the average critical current. Solid blue line: without defects. Orange dashed line: with defects.

coil to experimental results from [4], which studies a REBCO pancake coil under current ramping. In order to study local current distribution around defects in smaller coils, we simulate a 7-turn coil with defects.

A. *Validation of the Model*

First, we simulate an HTS tape with uniform I_c distribution (defect-free tape) and HTS tape containing defects in order to compare to experimental results obtained in [21]. The I_c of the defects is below 80% of the average I_c across the tape [21]. Hahn et al. found no measurable difference between the magnetic field generated by a 135-turn REBCO pancake coil with six significant defects and the theoretical magnetic field strength for a defect-free tape with uniform I_c distribution. Although Hahn's experiment uses a pancake coil with 135 turns, we simulated a 99-turn coil, due to the practical limitation of NGSPICE runtime, with six defects placed randomly throughout the tape. For each defect, the I_c was set to 34.1 A, 50% of the average I_c across the coil, 68.2 A. Our results, shown in Fig. 2, agree with Hahn's observation that for a many-turn coil with transport current less than the average I_c of the tape, the magnetic field produced by a coil with defects does not differ significantly from the magnetic field produced by a coil without defects. However, as we shall discuss later, our findings about current-sharing around defects suggest that "defect-irrelevancy" only holds for cases when the severity of the defect(s) is relatively low compared to the number of turns in a coil.

Fig. 3 shows the simulation results and the measurement data reported in [4]. A time-dependent thermal simulation while ramping the transport current from 0 to 100 A was performed. A qualitative agreement with the experimental results can be observed: the central magnetic field increases nearly linearly until the point when the transport current surpasses the initial characteristic tape I_c. Once the I_c in the tape has decreased to zero due to heating, the central magnetic field sharply collapses before reaching a stable minimum value resulting from the current flowing in the Cu stabilizer. In tandem, the voltage is

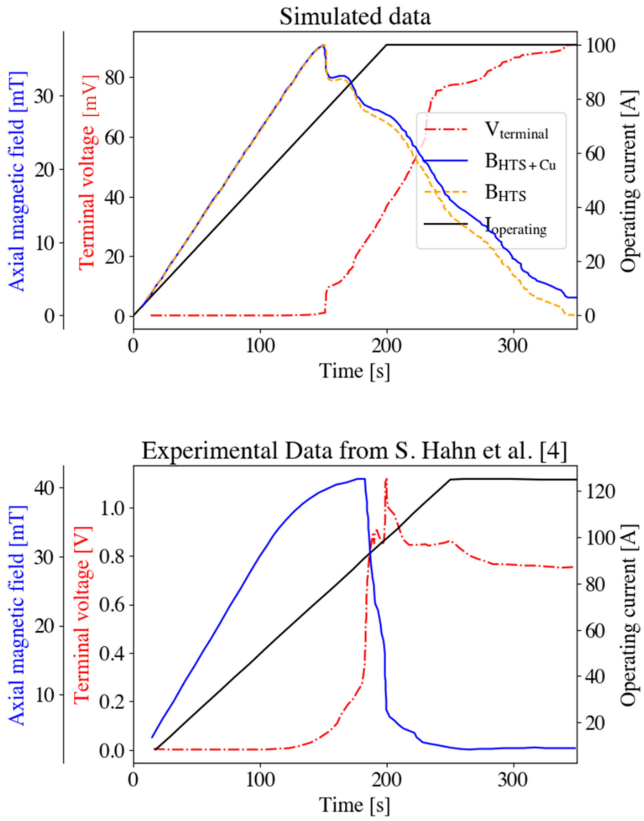

Fig. 3. Top: Simulated magnetic field (blue solid line representing total magnetic field, and orange dashed line representing magnetic field contribution from HTS layer only) and terminal voltage (red dashed line) for a 30-turn pancake coil with a transport current ramping from 0 to 100A (black, arbitrary scale). Bottom: Experimental [4] magnetic field (blue solid line) and terminal voltage (red dashed line) for a 30-turn pancake coil with a transport current ramping from 0 to 125A (black, arbitrary scale). In the simulation, the I_c of 68.2A is reached at about 150 s.

stable until the initial I_c is reached, after which the rate of increase in the voltage increases.

Although the simulated data capture the general behavior represented in the experimental data, a few discrepancies remain: first, the linear regime of the magnetic field in the simulated data extends further than the experimental magnetic field—until just before the magnetic field collapse. Second, the terminal voltage fluctuates for a period after reaching a local maximum and continues to increase after the period of fluctuation—a significant difference from the experimental voltage, which plateaus at a lower value than its peak. This discrepancy may be attributed to assumptions made by the model. Notably, our model assumes adiabatic conditions: all heat generated in the coil warms up the coil. In experiment, the coil is submerged in a bath of liquid nitrogen where heat exchange between the coil and cryogen occurs, contrary to the adiabatic assumption. To approximate heat dissipation due to cooling, we ran the simulation with heat contained within the coil scaled down to a percentage of the total heat generated in the coil. When only 10% of the heat generated in the coil was allowed to stay in the coil, we obtained

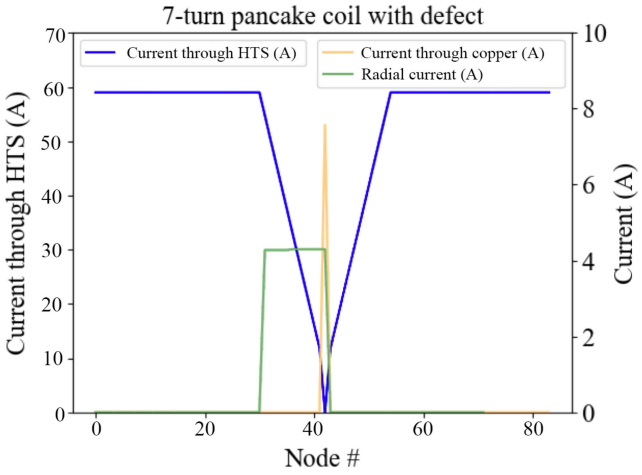

Fig. 4. Current distribution through each material layer in a pancake coil with a defect on the fourth turn with a critical current of 0 A. Current distribution in HTS (blue) drops almost linearly in the whole turn before the defect and recovers almost linearly in the whole turn after the defect. Radial current before the defect is constant and positive, indicating that current diverts outward to the next turn at a constant rate.

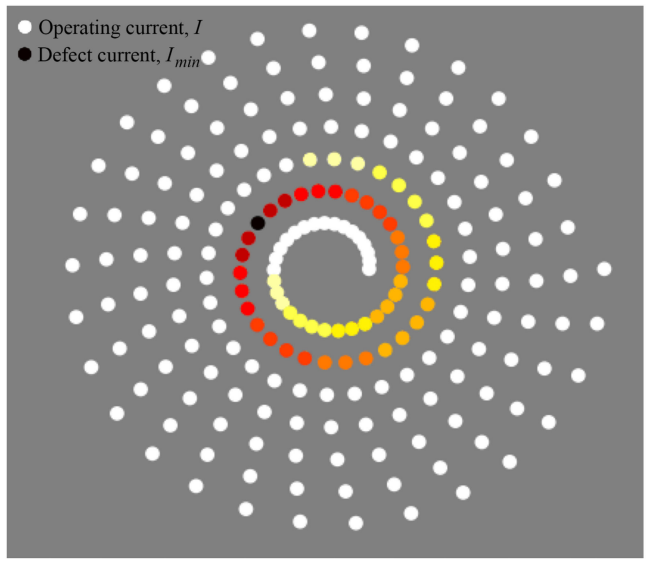

Fig. 5. A conceptual diagram showing the distribution of the current in each HTS section of a seven-turn pancake coil with a defect. Minimum current (critical current of the defect) is represented in black. Maximum current (operating current) is represented in white. The current increases as the color changes from black to brown, orange, yellow to white.

a magnetic field rise comparable to the slow increase as measured in [4]. This weighted thermal simulation approximates the effect of a liquid nitrogen bath that suppresses the temperature rise in the coil. Additionally, the terminal voltage drop that is observed in [4] is likely because the voltage contribution from inductance vanishes for constant current, causing a reduction in observed terminal voltage once the operating current has stabilized.

B. Insights Into Current Distribution Around Defects

Although work validating the model's thermal simulation remains, our results offer insights into current sharing behavior around local I_c defects. As illustrated by Fig. 1 in [21], a common thought is that current might bypass a defect or local normal zone, flowing radially around it before merging back into the turn containing the defect or normal zone. However, results from our model for a 7-turn coil with 12 sections per turn, shown in Figs. 4 and 5, suggest that current evacuates from the entire turn containing the defect and flows radially at a constant rate into neighboring turns. In other words, the current in the superconducting layer of the turn decreases linearly to the I_c of the defect in the turn before and recovers back to the transport current in the turn after (Fig. 5). This behavior indicates that a significant defect disrupts current flow through two full turns (Fig. 5). The behavior is contrary to the illustration in [21] where the current sharing completes locally around a defect. It also suggests that the impact of a defect on the function of the coil is relative to the location of defects, size of the coil, the number of turns, and severity of the defect in terms of I_c. For example, a single severe defect in each of six neighboring turns would disrupt azimuthal current flow in eight turns, while six severe defects along one turn of the coil would disrupt just more than two turns of the coil. In both cases, the impact of such disruptions depends on the size of the coil and the severity of the defects, but the distribution of defected sites in the latter case is generally less disruptive than in the former.

IV. Conclusion

We report insights into current sharing behavior in a REBCO pancake coil using an electrical network model that takes into account the local heat generation and temperature rise in the coil under adiabatic conditions. Comparison with published experimental data confirms that this model captures the essential behavior of the pancake coil system. Results of this model reported here offer initial insights into the distributions of heat and current in a no-insulation REBCO pancake coil. In particular, our model suggests that the assumption that current bypasses a defect and merges back into the defect's turn can be incorrect: the current flows radially from the turn before the defect into the turn after the defect, thereby disrupting the azimuthal current in two full turns. This finding suggests that defect irrelevancy can be relative to the severity of the defects, the size of the coil, and the distribution of defects within the coil. Further studies in development of REBCO magnet technology should account for this behavior. In addition, heat generation due to current sharing in a no-insulation coil or cable should be considered, in particular for conduction-cooled magnet applications [22]. The model may be used to study the impact of electrical contact resistances between conductor turns to regulate current sharing [18].

A few areas for improvement remain, including a better description of the heat transfer between the coil and environment and including coil inductance to study non-dc situations.

REFERENCES

[1] D. Larbalestier, A. Gurevich, D. M. Feldmann, and A. Polyanskii, "High-Tc superconducting materials for electric power applications," *Nature*, vol. 414, no. 6861, pp. 368–377, 2001.

[2] X. Wang, S. A. Gourlay, and S. O. Prestemon, "Dipole magnets above 20 tesla: Research needs for a path via high-temperature superconducting REBCO conductors," *Instruments*, vol. 3, no. 4, 2019, Art. no. 62.

[3] S. van, W. Steven, and K. R. Marken, "Superconducting magnets above 20 tesla," *Phys. Today*, vol. 55, no. 8, pp. 37–42, 2002. [Online]. Available: https://doi.org/10.1063/1.1510280

[4] S. Hahn, D. K. Park, J. Bascunan, and Y. Iwasa, "HTS pancake coils without turn-to-turn insulation," *IEEE Trans. Appl. Supercond.*, vol. 21, no. 3, pp. 1592–1595, Jun. 2011, doi: 10.1109/TASC.2010.2093492.

[5] S. Hahn *et al.*, "45.5-Tesla direct-current magnetic field generated with a high-temperature superconducting magnet," *Nature*, vol. 570, no. 7762, pp. 496–499, Jun. 2019. [Online]. Available: https://doi.org/10.1038/s41586-019-1293-1

[6] R. Gyuráki, T. Benkel, F. Schreiner, F. Sirois, and F. Grilli, "Fluorescent thermal imaging of a non-insulated pancake coil wound from high temperature superconductor tape," *Supercond. Sci. Technol.*, vol. 32, no. 10, 2019, Art. no. 105006. [Online]. Available: https://doi.org/10.1088/1361-6668/ab38f2

[7] Y. Wang, H. Song, D. Xu, Z. Y. Li, Z. Jin, and Z. Hong, "An equivalent circuit grid model for no-insulation HTS pancake coils," *Supercond. Sci. Technol.*, vol. 28, no. 4, 2015, Art. no. 045017. [Online]. Available: https://doi.org/10.1088/0953-2048/28/4/045017

[8] X. Wang, T. Wang, E. Nakada, A. Ishiyama, R. Itoh, and S. Noguchi, "Charging behavior in no-insulation REBCO pancake coils," *IEEE Trans. Appl. Supercond.*, vol. 25, no. 3, Jun. 2015, Art. no. 4601805. [Online]. Available: https://doi.org/10.1109/TASC.2014.2365623

[9] X. Wang *et al.*, "Turn-to-turn contact characteristics for an equivalent circuit model of no-insulation ReBCO pancake coil," *Supercond. Sci. Technol.*, vol. 26, no. 3, 2013, Art. no. 035012. [Online]. Available: https://doi.org/10.1088/0953-2048/26/3/035012

[10] Y. Suetomi, K. Yanagisawa, H. Nakagome, M. Hamada, H. Maeda, and Y. Yanagisawa, "Mechanism of notable difference in the field delay times of no-insulation layer-wound and pancake-wound REBCO coils," *Supercond. Sci. Technol.*, vol. 29, no. 10, 2016, Art. no. 105002. [Online]. Available: https://doi.org/10.1088/0953-2048/29/10/105002

[11] E. Ravaioli, "CLIQ, a new quench protection technology for superconducting magnets," Ph.D. dissertation, Univ. Twente, 2015. [Online]. Available: https://doi.org/10.3990/1.9789036539081

[12] A. V. Gavrilin, D. J. Kolb-Bond, K. L. Kim, K. Kim, W. S. Marshall, and I. R. Dixon, "Quench and stability modelling of a metal-insulation multi-double-pancake high-temperature-superconducting coil," *IEEE Trans. Appl. Supercond.*, vol. 31, no. 5, Aug. 2021, Art. no. 4601707.

[13] A. V. Dudarev *et al.*, "Superconducting windings with 'short-circuited' turns," *Proc. Inst. Phys. Conf. Ser.*, vol. 158, pp. 1615–1618, 1997.

[14] K. R. Bhattarai *et al.*, "Understanding quench in no-insulation (NI) REBCO magnets through experiments and simulations," *Supercond. Sci. Technol.*, vol. 33, no. 3, 2020, Art. no. 035002.

[15] S. Noguchi, "Electromagnetic thermal and mechanical quench simulation of NI REBCO pancake coils for high magnetic field generation," *IEEE Trans. Appl. Supercond.*, vol. 29, no. 5, Aug. 2019, Art. no. 4602607.

[16] W. D. Markiewicz, J. J. Jaroszynski, D. V. Abraimov, R. E. Joyner, and A. Khan, "Quench analysis of pancake wound REBCO coils with low resistance between turns," *Supercond. Sci. Technol.*, vol. 29, no. 2, 2016, Art. no. 025001.

[17] A. C. A. Martínez, Q. Ji, S. O. Prestemon, X. Wang, and G. H. I. Maury Cuna, "An electric-circuit model on the inter-tape contact resistance and current sharing for REBCO cable and magnet applications," *IEEE Trans. Appl. Supercond.*, vol. 30, no. 4, Jun. 2020, Art. no. 6600605.

[18] Z. Yang, A. C. A. Martínez, S. V. Muley, X. Wang, Q. Ji, and A. Anders, "Vanadium oxide coatings to self-regulate current sharing in high-temperature superconducting cables and magnets," *J. Appl. Phys.*, vol. 128, no. 5, 2020, Art. no. 055105. [Online]. Available: https://doi.org/10.1063/5.0013783

[19] NGSPICE, version 36, 2021. [Online]. Available: https://ngspice.sourceforge.io/

[20] J. van Nugteren, "Normal zone propagation in YBCO superconducting tape," M.S. thesis, Univ. Twente, 2012. [Online]. Available: http://essay.utwente.nl/62096/1/MSc_J_van_nugteren.pdf

[21] S. Hahn *et al.*, "Defect-Irrelevant' behavior of a no-insulation pancake coil wound with REBCO tapes containing multiple defects," *Supercond. Sci. Technol.*, vol. 29, no. 10, Sep. 2016, Art. no. 105017, doi: 10.1088/0953-2048/29/10/105017.

[22] U. Bong, J. Kim, J. Bang, J. Park, K. J. Han, and S. Hahn, "'Defect-irrelevant-winding' no-insulation (RE)$Ba_2Cu_3O_{7-X}$ Pancake coil in conduction-cooling operation," *Supercond. Sci. Technol.*, vol. 34, no. 8, 2021, Art. no. 085003. [Online]. Available: https://doi.org/10.1088/1361-6668/ac0759